# DEVELOPING OPTICAL MEASUREMENT TECHNIQUES FOR IMPROVING IGNITION SIMULATION MODELS

***Saraschandran Kottakalam*[1], *Ahmad Anas Alkezbari*[2], *Gregor Rottenkolber*[1], *and Christian Trapp*[2]**

[1] ***Esslingen University of Applied Sciences***
[2] ***University of the Bundeswehr Munich***
*saraschandran.kottakalam@hs.esslingen.de*

## Abstract

Computational Fluid Dynamics (CFD) simulations are an important part of the development of new combustion strategies and innovative powertrain concepts. Since the ignition model initiates combustion in CFD simulation models of spark-ignited engines, it is crucial to have an ignition model that accurately represents the phenomena. Therefore, it is essential to have a fundamental physical understanding of ignition phenomena in order to optimise spark-ignited engines to meet customer expectations and regulatory requirements. This study presents new experimental/measurement techniques developed with a focus on validating and improving existing ignition simulation models. These newly developed tests are used to observe sparks in an optically accessible flowbench capable of reproducing engine operating conditions. Through these tests, spark parameters such as spark elongation and phenomena such as the interaction of the spark with the surrounding medium have been observed and quantified. The knowledge gained was used to calibrate and improve an existing ignition simulation model.

## 1 Introduction

To meet new legislation and customer expectations, internal combustion engines (ICEs) running on renewable fuels need to be further developed with a focus on efficiency and emissions. Computational Fluid Dynamics (CFD) plays an important role in the design and development of these new ICEs. Predictive simulations allow many design approaches and optimisations to be quickly calculated without the use of real components or test benches. However, they must be calibrated and validated to represent the physical processes as accurately as possible. This can only be done using measurement techniques that provide insight into these phenomena to model, improve and validate the simulation models.

In the case of a spark-ignited engine, ignition plays a significant role in the combustion characteristics and it needs to be accurately represented by the simulation models. In the development of innovative engine concepts, such as ultra-lean hydrogen engines or engines with prechamber spark plugs, a deep understanding of ignition phenomena is key to both improving simulation models and achieving consistent ignition. However, research has shown that most combustion models use simplified versions of ignition and/or bypass the ignition model and go directly to the combustion part by introducing an initial flame kernel (tunable) as explained by Schaefer (2016). Although this was acceptable for the development of older generation engines, the challenging operating conditions of the new combustion concepts require novel measurement techniques to provide further insight into ignition phenomena. Examples include ultra-lean operation (lower probability of having a combustible mixture at the ignition source) and prechamber ignition (less volume around the ignition source, high probability of flame quenching).

The focus of this study is to develop innovative optical measurement techniques that can provide insight into ignition phenomena in spark-ignited engines and provide quantifiable parameters for the development and validation of ignition simulation models. The optical measurement techniques developed in this study will be used to analyse not only the influence of flow field on the spark behaviour, but also the influence of the spark on the flow field.

## 2 Experimental investigation

The experiments were carried out in a wind tunnel testbed specifically designed to test sparks under real engine conditions. This testbed has optical access through two glass windows. The spark plug orientation can be varied by means of the upper flange of the optical chamber. The testbed is designed for operations with non-combustible mixtures upto a pressure of 40 bar, temperature of 473 K and a maximum flow velocity of 40 m/s. A detailed schematic of the wind tunnel can be seen in Figure 1.
A standard J-gap spark plug was used for the development of the measurement techniques, powered by a Bosch variable ignition system. The sparks produced were captured at speeds of up to 300,000 fps using a Photron FASTCAM SA-X2 with a CMOS sensor capable of detecting emissions in the 400-1000 nm range. The secondary voltage and current of the ignition system were also measured by means of Tekro-

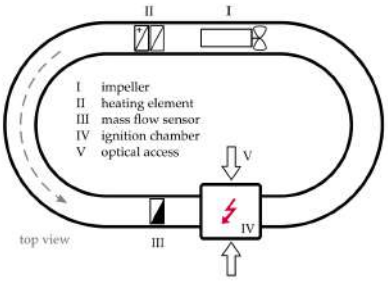


Figure 1: Schematic of the spark windcanal testbed Wörner and Rottenkolber (2021)

nix P6015A and FOS OCS 1000 probes respectively. These measurements were recorded with an oscilloscope (Yokogawa DLM4038). The tests were performed with standard induction coil discharge of 32 mJ energy measured at the secondary coil.

### Plasma channel

In order to get the plasma parameters, the images of the plasma channel taken by the high-speed cameras were processed by a Matlab algorithm. This in-house developed algorithm is capable of detecting the spark in each frame and obtain the length, diameter and volume of the spark. Other relevant information such as the occurrence of restrikes and short-cuts, as well as the shape and location of the spark at different times, also provide further insight into the physics of sparks.

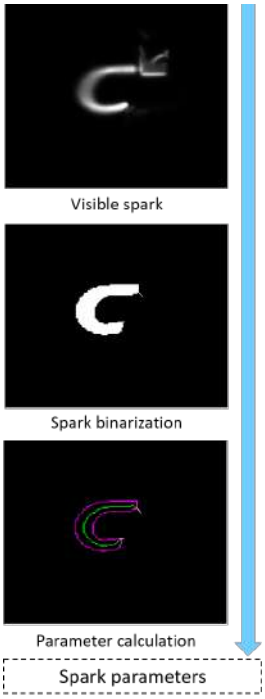


Figure 2: Processing steps of the matlab algorithm (flow from right to left)

In combination with the electrical measurements, the energy present in the spark can also be calculated. This can be correlated to the heat transfer to the surrounding, which is an important parameter for the ignition simulation model.

### Heat transfer

The heat transfer from the spark to the environment is also critical to understanding the phenomenon of spark ignition. Visualisation of the density gradient has been difficult due to the extremely high temperatures associated with sparks and the very short time scale of spark formation. So, an existing measurement technique was adopted and optimized for this application.

**Background Oriented Schlieren (BOS).** Background Oriented Schlieren (BOS) is a measurement technique used to visualise and quantify density gradients. It works on the principle that light rays are refracted as a result of varying refractive indices caused by changes in the density of a medium. In BOS, algorithms capable of detecting minute changes in two images are utilized. These algorithms calculate the displacement/deformation of a background pattern captured through a density gradient by a camera. BOS is extensively used for visualizing density gradients due to its relatively simple experimental setup as documented by Raffel (2015). Wildeman (2018) introduced the BOS technique, Fast Checkerboard Demodulation (FCD), which uses an algorithm that calculates the displacement vectors from the deformation of periodic background patterns. Shimazaki et al. (2022) also mentions the advantages of FCD compared to some of the other techniques like PIV algorithm, like the faster computation with the same resolution as the raw images and not having to take into account the additional parameters such as interrogation windows as used in some PIV techniques .

The displacement detected by the BOS algorthm is proportional to the change in refractive index and the density as mentioned by Venkatakrishnan and Meier (2004) in equation (1).

$$\frac{\partial^2 \rho((x,y))}{\partial x^2} + \frac{\partial^2 \rho((x,y))}{\partial y^2} = S\,(x,y) \qquad (1)$$

Where :

$\rho$ = density of the medium
$\delta x$ = displacement in the horizontal axis
$\delta y$ = displacement in the vertical axis

S(x,y) in equation (1) is calculated from the displacement detected by BOS algorithms. Numerical integration of the Poisson equation would yield the refractive index of the flowfield. The refractive index of a medium is related to the density by the Gladstone-Dale constant as shown in equation (2) and then the temperature of the medium can also be calculated according to equation (3). These calculations are

based on the assumption that in the case of sparks, the pressure is constant and therefore the refractive index changes are solely caused by temperature differences.

$$\rho = \frac{n-1}{K} \tag{2}$$

Where:

$\rho$ = density of the medium
$n$ = refractive index of the medium
$K$ = Gladstone-Dale const. (wavelength dependent)

$$T = \frac{p}{\rho R} \tag{3}$$

Where:

$T$ = temperature
$p$ = pressure

**Forward Projected Background Oriented Schlieren.** The sparks generate very high density gradients due to the high temperatures of the plasma column in a relatively small volume. This poses some challenges for existing BOS techniques. Since the expected density gradients are really high, larger patterns have to be used, because if it is small they will blurr the pattern and ultimately lead to poor results. Using larger patterns also reduces the resolution of the measurement as the smaller the pattern, the higher the resolution and vice versa. Another way to overcome this issue is to weaken the BOS signal. The sensitivity of the BOS decreases the closer the pattern is to the density gradient. However, there is a limit to the placement of the pattern as it can affect the flow and it is not possible to have it inside the test bed due to design restrictions.

As a solutin, a new BOS technique has been developed that can be used for detailed visualisation of high density gradients. In this new technique, instead of a printed background pattern placed behind the density gradient (with respect to camera), the background is projected into the focal plane of the camera (or directly onto the sensor). This is extremely advantageous as it allows the background pattern to be in the desired plane within the focus range of the camera lens without disturbing the flow field. A detailed schematic of the experimental setup for the new Forward Projected BOS technique is shown in Figure 3.

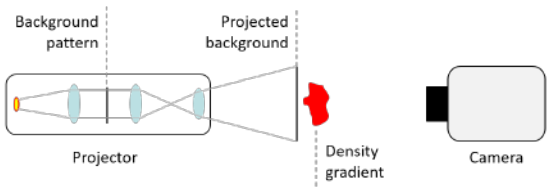


Figure 3: Experimental setup for Forward Projected BOS

## 3 Simulation

In order to check the spark movement and quenching effect near the wall, as well as the first flame kernel formation, a good physical-based ignition model is required. For this study, AVL-CADIM "Curved Arc Diffusion Ignition Model", the most advanced ignition model in AVL FIRE M was used, and the sub-models for this model will be discussed in more depth in this section.

**AVL-CADIM ignition model**

The AVL-CADIM ignition model is made up of four sub-models: the spark channel model, the electrical circuit model, the ignition delay model, and the initial kernel growth model, which are all based on ideas published by Schaefer (2016).

1. Spark channel: A proper description of the spark channel and its deflection during 3D engine simulation is the goal of the spark channel sub-model. The hot plasma composed of gas atoms, ions, and molecules forms the visible channel between the spark electrodes at the moment of breakdown. This plasma channel can be dragged by the local flow field surrounding the spark plug, and its length and shape are significantly altered. AVL (2022) documents that the spark channel is an evolving 3D curve with discrete Lagrangian particles as its representation.

2. Electrical circuit: The secondary electrical circuit model as in the so-called AKTIM model described by Duclos and Colin (2001) is used to calculate the amount of energy delivered to the spark plasma channel. Accordingly, the energy transfer to the hot plasma column is calculated as follows:

$$\dot{Q_{gc}} = V_{gc} \,.\, i_s \tag{4}$$

Where:

$\dot{Q_{gc}}$ = energy delivered to the plasma channel
$V_{gc}$ = voltage in gas column
$i_s$ = secondary current

A restrike occurs when the breakdown voltage is reached by the interelectrode voltage and a new spark channel forms between the electrodes and replaces the current one. A single spark discharge event may have several restrikes, depending on the energy in the secondary circuit. It is also worth noting that although some energy may still be available in the circuit, the calculation of spark channel movement and secondary electrical circuit is stopped and spark particles are suppressed in the event of successful ignition as documented in AVL (2022).

3. Ignition delay: Although plasma temperatures are far too high for normal combustion products

to exist, combustion reactions take place at the outer surface of the plasma, where conditions are ideal for rapid chemical activity (temperatures ranging from thousand to a few thousand Kelvin) as documented by Heywood (1988).

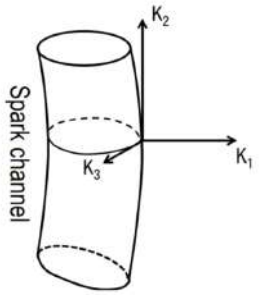


Figure 4: K-coordinate system

This is the primary assumption for AVL-CADIM's ignition delay time sub-model. As explained by Schaefer (2016), the temperature at the surface of the spark channel is obtained by deriving and solving the 1D heat equation with curvature terms in the K-coordinate system shown in Figure 4.

Equation (5) expresses the temperature equation solved in the K1-domain. Equation (6) describes the heat transfer from the spark toward the K1-domain with a Neumann boundary condition as a temperature gradient at the surface of the spark channel.

$$\rho\frac{\partial T}{\partial t} = \frac{\partial}{\partial K}\left(\frac{\lambda}{c_p}\frac{\partial T}{\partial K}\right) - K_\beta\frac{\lambda}{c_p}\frac{\partial T}{\partial K} + \frac{\lambda}{c_p^2}\frac{\partial c_p}{\partial K}\frac{\partial T}{\partial K} + \frac{1}{c_p}\frac{\partial p}{\partial t} \tag{5}$$

Where:

$K_\beta$ = sum of curvatures in tangential direction
$\lambda$ = thermal conductivity
$c_p$ = specific heat capacity at const. pressure

$$\left.\frac{\partial T}{\partial K}\right|_{K_1=0} = \frac{\dot{Q_{gc}} \cdot \eta_{eff}}{\lambda \,.\, A_{spk}} \tag{6}$$

Where:

$\eta_{eff}$ = efficiency of spark heat transfer
$A_{spk}$ = area of the spark channel surface

An ignition delay time ($\tau$) is obtained from a database for the temperature calculated at the surface of the spark plasma and the local mixture composition. For a given ignition delay time, an instantaneous change in ignition precursor, $dY_p$, is calculated with the model proposed by Francois et al. (2002). For each particle representing the spark, the precursor value (starting from 0) is calculated and when it reaches 1.0, an initial flame kernel is formed at that location, as shown in Figure 5.

4. Initial kernel growth: Once the initial flame kernel is formed, a 0D model is used to model its early growth, as this size may be too small to be resolved by the combustion model on the 3D mesh. Equation (7) is used to determine the expansion speed of the kernel, where $\rho_u$ and $\rho_b$ are the unburned and burned densities, respectively and $s_K$ is the burning velocity at the surface of the kernel. Equation (8) uses the laminar burning velocity ($s_L$) obtained from the FIRE™ M database for a given mixture composition and properties, the turbulent flame speed ($s_T$), and the turbulent diffusivity ($D_t$) to calculate the burning velocity at the surface of the kernel ($s_K$).

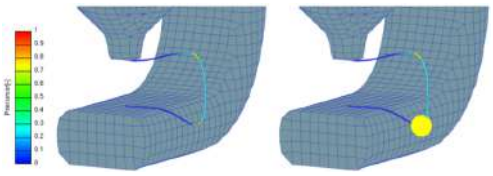

Figure 5: Spark precursor and initial flame kernel AVL 2022

$$\frac{dr_K}{dt} = \frac{\rho_u}{\rho_b}s_K \tag{7}$$

$$s_K = max\left(s_L, s_T - \frac{2}{r_K}D_t\right) \tag{8}$$

For the simulation, a polyhedral mesh was used because the gradient can be well approximated with such a mesh (the cell has many neighbours), the global mesh cell size is 1 mm with a mesh refinement near the spark plug gap (cell size is 0.2 mm), Figure 6 shows a cross-section of the mesh. Using the RANS approach, the turbulence model used is k-zeta-f and the combustion model used is ECFM3Z.

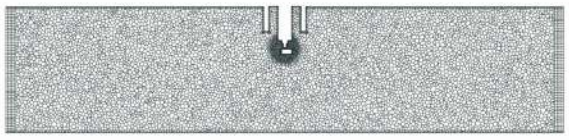

Figure 6: Cross-section of the CFD mesh

Since the ignition model is a transient model, the simulation is also a transient simulation. In this case, the flow converged and had a steady flow pattern after

0.3 seconds from the start of the simulation, and the spark model is not activated until the flow is steady.

## 4 Results and validation

The results obtained from the experimental measurements were used to compare and validate the simulation model. Figure 7 shows a comparison of the spark length (averaged over 10 spark events) and the spark lengths calculated by the AVL-CADIM model. The tests in the testbed were performed at atmospheric pressure and at a flow velocity of 10 m/s and the simulation results were obtained after calibrating the ignition model to achieve good agreement of spark length till the second restrike.

The results in Figure 7 demonstrate the ability of

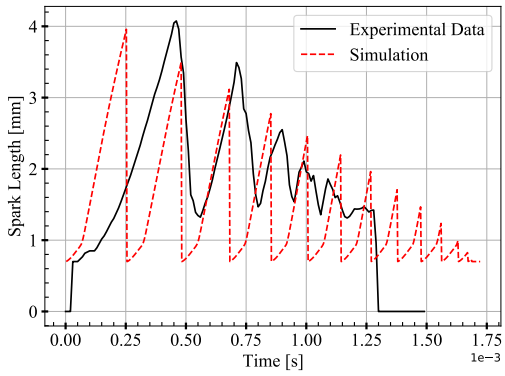


Figure 7: Spark length validation for the AVL-CADIM ignition model

the AVL-CADIM model to simulate multiple spark restrikes. It was observed that the spark in simulation activates immediately at the trigger of ignition. However, in the test bench, there exists a delay and the break down occurs approximately 0.04 ms after the trigger. It was also observed that the first re-strike in the simulation occurs approximately 0.21 ms earlier than in the test bed and the comparison of the spark shape in Figure 8 shows the same effect. The spark in the simulation is stretched slightly more than the test bench at two different time steps (0.05 and 0.1 ms) after the breakdown in both cases (compensated for the delay). It was also observed that in the simulation the spark lasted longer and that the sparks were confined to movement in the horizontal plane of the electrodes.

Figure 9 shows a result from the Forward Projected BOS. The flow is from right to left and the highest flow heating was observed downstream of the mass electrode. It can be seen that the heated volume is significantly larger than the plasma channel. In addition to this, the effect of the spark on the flow field was also observed. Since the spark is slower than the flow (especially between the spark gaps), BOS provides a way to observe the flow field as well as the spark and understand the spark-flowfield interaction better.

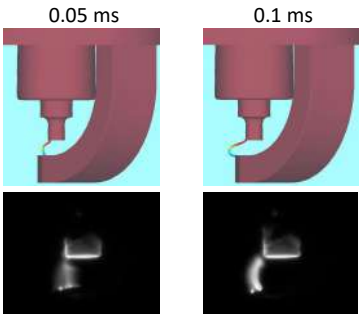


Figure 8: Spark shape validation for the AVL-CADIM ignition model in the 3D domain

It is worth noting that the test was performed at a 100,000 fps and at an absolute pressure of 6 bar. Under these conditions, it was not possible to obtain usable results from previously existing BOS techniques. However, with Forward Projected BOS, the density gradients generated by the spark through heat transfer to the surrounding can be visualised at high resolution. Figure 9 shows the heat transfer from spark obtained through numerical integration of Poisson equation (1). It has to be pointed out that no quantitative temperatures are shown because it was not possible to calibrate and validate the system up to now. Crucial is the low temporal resolution of standard temperature measurement systems. So work has to be done to develope a calibration/validation set up.

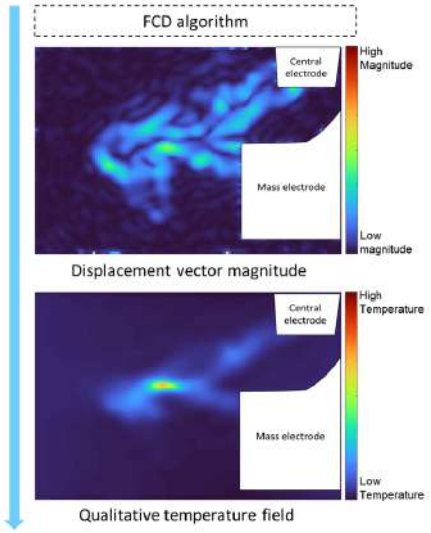


Figure 9: Heat transfer visualisation with Forward Projected BOS

The insights gained from studies mentioned in this paper were also used to calibrate the AVL-CADIM ignition model used in full engine simulation. Validation studies of the pressure curve and cumulative heat release in a gasoline single cylinder research engine using the calibrated AVL-CADIM ignition model are

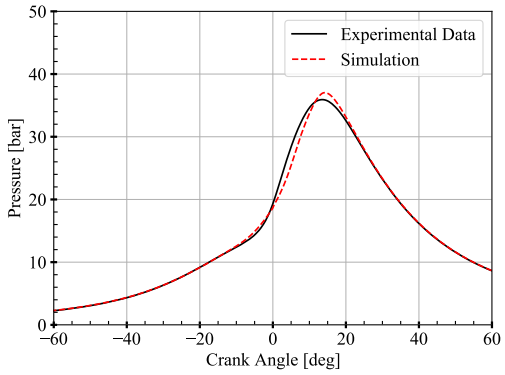


Figure 10: Pressure in the engine cylinder

shown in Figures 10 and 11 respectively. It is clear from the excellent matching of pressure and cumulative heat release slightly after the ignition angle that the simulation of ignition behavior in pressure and cumulative heat release curves show very good agreements with the experimental results.

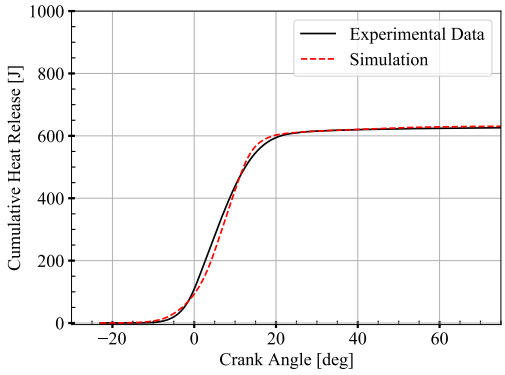


Figure 11: Cumulative heat release in the engine cylinder

## 5 Conclusions

The combination of measurement techniques described in this paper can be used to gain a comprehensive and detailed understanding of spark ignition phenomena. These measurement techniques provide an important correlation between the volume of the plasma channel and the heated volume of the flow medium. As demonstrated, the insights gained through the studies performed so far has lead to improvement in simulation results. The results presented also validates the motivation for conducting this study.

## 6 Outlook

The measurement techniques described in this paper results in a unique approach, which will be further developed. The Forward Projected BOS technique will be further optimized and calibrated to obtain temperature measurement around the spark with a goal of estimating the location of the first flame kernel. This facilitates the further development of ignition simulation models through incorporation of the spark as an ignition source leading to initial kernel formation. Rather than the common approach of directly using a simplified spherical flame kernel and ignoring the spark phase, the accuracy of combustion simulation in internal combustion engines can be improved. These improvements would be performed in parallel with validation in engines aimed at developing innovative drivetrain solutions.

## Acknowledgments

This work was funded by dtec.bw. dtec.bw is funded by the European Union – NextGenerationEU. The authors gratefully acknowledge the provision of licenses for the AVL Simulation Suite by AVL Deutschland GmbH.
Additionally, the authors thank the colleagues from the University of the Bunderswehr Munich, Mr. Rudolf Höß and Mr. Pravin Kumar Sundaram for performing the experimental investigations in the engine.
The authors also gratefully acknowledge the help of colleagues from Esslingen University of Applied sciences, Mr. Christoph Spang, Mr. Tim Schwellinger and Mr. Samuel Prendergast.

## References

AVL List GmbH(2022), FIRE™ M User Manual: R2022.1, *AVL Documentation*.

Duclos, J.M. and O Colin (2001), Arc and Kernel Tracking Ignition Model for 3D Spark-Ignition Engine Calculations.

Francois, Lafossas, Michel Castagne, J. Dumas, and S. Henriot (Oct. 2002), Development and Validation of a Knock Model in Spark Ignition Engines Using a CFD code.

Heywood, J. B (1988), Internal Combustion Engine Fundamentals.

Raffel, Markus (Mar. 6, 2015), Background-oriented schlieren (BOS) Techniques,*Springerlink.com*.

Schaefer , L. (2016), Modeling and Simulation of Spark Ignition in Turbocharged Direct Injection Spark Ignition Engines, *Ph.D. Dissertation, TU Bergakademie Freiberg*.

Shimazaki, Takaaki, Sayaka Ichihara, and Yoshiyuki Tagawa (2022), Background oriented schlieren technique with fast Fourier demodulation for measuring large density-gradient fields of fluids, *Experimental Thermal and Fluid Science 134*, p. 110598.

Venkatakrishnan, Lakshmi and Meier, G. (2004), Density Measurements Using the Background Oriented Schlieren Technique, *Experiments in Fluids*. 37. 10.1007/s00348-004-0807-1.

Wildeman, Sander (May 16, 2018), Real-time quantitative Schlieren imaging by fast Fourier demodulation of a checkered backdrop, *Experiments in Fluids* 59.

Wörner, Michael and Gregor Rottenkolber (2021), Voltage rise anemometry in turbulent flows applied to internal combustion engines,*Experiments in Fluids* 62.132 (6).